Polycyclic Aromatic Hydrocarbon for the Detection of Nonpolar Analytes under Counteracting Humidity Conditions

Nadav Bachar,[†,‡] Lena Mintz,[†,‡] Yael Zilberman,[†,‡] Radu Ionescu,[†,§] Xinliang Feng,[⊥] Klaus Müllen,[⊥] and Hossam Haick*,[†]

[†]The Department of Chemical Engineering and the Russell Berrie Nanotechnology Institute, Technion — Israel Institute of Technology, Haifa 32000, Israel

[§]The Department of Electronics, Electrical and Automatic Engineering, Rovira i Virgili University, 43007 Tarragona, Spain

[⊥]Max-Planck-Institute for Polymer Research, Postfach 3148, D-55021 Mainz, Germany

S *Supporting Information*

ABSTRACT: Real-world samples contain reducing and oxidizing chemical agents as well as large and small (bio)molecules, which are polar or nonpolar in nature. Sensing nonpolar analytes, which is of paramount importance for a wide variety of applications, is generally more difficult to achieve than sensing polar analytes. Here, we report on empirical observations of a unique polycyclic aromatic hydrocarbon derivative, referred as PAH-A, whose structure has a triangular-shaped aromatic core (with a carbon number of 60) and contains hydrophobic mesogens terminated with hydrophobic alkyl chains. We show that films made of PAH-A enable excellent sensitivity to nonpolar analytes, compared to polar analytes, in a setting of 5−40% counteracting relative humidity. This finding is based on monitoring the changes in the physical/optical properties of thin PAH-A films upon exposure to nonpolar and polar analytes, by means of quartz crystal microbalance and spectroscopic ellipsometry measurements. A comparison with other polycyclic aromatic hydrocarbon derivatives with different cores or organic functionalities is provided and discussed.

KEYWORDS: *polycyclic aromatic hydrocarbon, sensor, detection, nonpolar, polar, humidity*
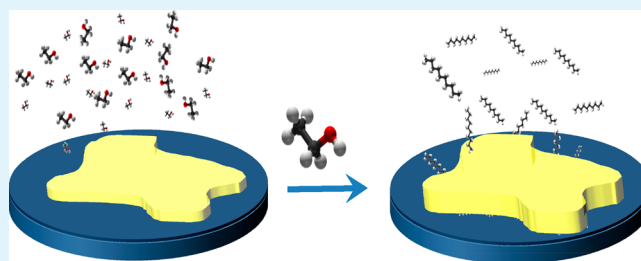
1. INTRODUCTION

Real-world samples contain reducing and oxidizing chemical agents as well as large and small (bio)molecules, which are polar and/or nonpolar in nature.[1] Sensing nonpolar analytes, which serve among the rest as diagnostic markers of various diseases,[2−8] is generally more difficult to achieve than sensing polar analytes.[1,9,10] Polar analytes are usually detected directly through charge exchange between the sensing material and the analyte,[1,9,11−13] and chemical selectivity of polar analytes is achieved through covalent functionalization with suitable organic molecules that interact strongly with the targeted analyte(s).[1,14−16] Nonpolar analytes, on the other hand, have to be detected indirectly via dielectric effects[11,12] or via steric interaction between the sensing material and the analyte (e.g., film swelling due to analyte adsorption), which might alter the transport of specific physical properties, such as charge carrier or optical wavelength.[1,4,5,14] Nevertheless, the interaction of the nonpolar analytes with sensing materials under real-world conditions is still hindered by weak to moderate selectivity and, also, by high and/or nonconstant humidity levels present in the environment and/or targeted sample.[17−20]

Recently, we have shown that an array of cross-reactive chemiresistive bilayers of single-wall carbon nanotubes and polycyclic aromatic hydrocarbons (PAHs),[18−20] in conjugation with sophisticated pattern recognition methods, provides >90% classification accuracy between polar and nonpolar analytes.[18] While promising, the use of sensor arrays requires increased power consumption and employment of sophisticated and time-consuming pattern recognition algorithms for data analysis and interpretation. A single, standalone sensor that can detect nonpolar analytes under counteracting humidity conditions would have major scientific and technological benefits.

In this paper, we report on a unique PAH derivative, referred as PAH-A, whose structure has a triangular-shaped aromatic core (with a carbon number of 60) and contains hydrophobic mesogens terminated with hydrophobic alkyl chains — see Figure 1 and Table 1. We show that films made of PAH-A enable excellent detection of nonpolar analytes from polar analytes at various counteracting humidity levels. This finding is based on monitoring the changes in the physical/optical properties of PAH-A thin film (see Figure 1 and Table 1) upon exposure to representative nonpolar analytes (decane, octane, hexane, dibutylether, and mestylene) and, for the sake of comparison, upon exposure to polar analytes (decanol, octanol,
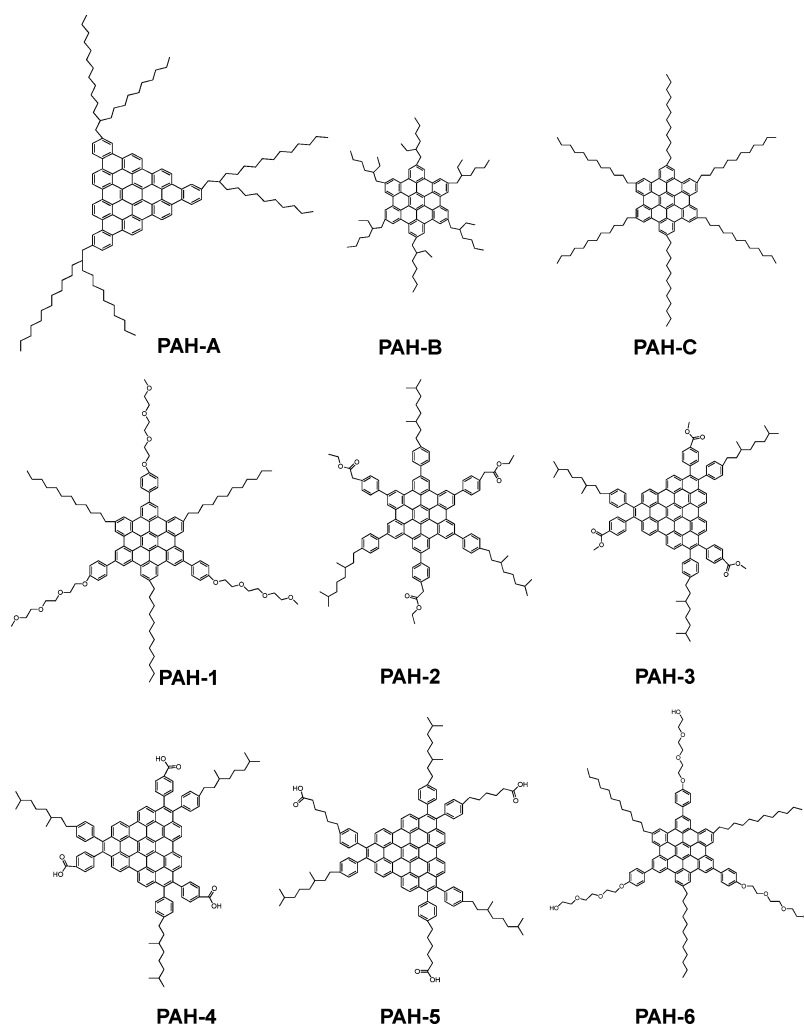
Figure 1. Structures of the PAH derivatives used in the current study; see Table 1.

Table 1. Main Structural Properties of the PAH Derivatives Used in the Experiments

PAH	corona core shape	number of carbon atoms in corona	side-group termination	side-group type
PAH-A	triangular	60	alkyl chain	nonpolar
PAH-B	hexagonal	42	alkyl chain	nonpolar
PAH-C	hexagonal	42	alkyl chain	nonpolar
PAH-1	hexagonal	42	ether (methyl)	weak polar
PAH-2	hexagonal	42	ester (ethyl)	strong polar
PAH-3	semi-triangular	48	ester (methyl)	strong polar
PAH-4	semi-triangular	48	carboxyl	strong polar
PAH-5	semi-triangular	48	carboxyl	strong polar
PAH-6	hexagonal	42	alcohol (hydroxyl)	strong polar

hexanol, and ethanol), under different relative humidity (RH) levels, by means of spectroscopic ellipsometry (SE) and quartz crystal microbalance (QCM) − NOTE: RH is defined as the ratio of the partial pressure of water vapor in the air−water mixture to the saturated vapor pressure of water at the prescribed temperature. The unique sensing properties of the PAH-A are compared with PAH derivatives having carbon corona of different shapes and sizes and terminated with either

hydrophobic or hydrophilic functional substituents (PAH-B, PAH-C, and PAH-1 to PAH-6; cf. Figure 1 and Table 1).

2. EXPERIMENTAL SECTION

Properties of PAH Derivatives. Figure 1 and Table 1 summarize the main structural properties of the PAH derivatives used in this study. The synthesis of PAH-A,[21] PAH-B,[22] PAH-C,[22] PAH-1,[23] and PAH-2[24] has been described in previous reports, whereas the synthesis of PAH-3 to PAH-6 will be reported elsewhere. These PAH derivatives contain hydrophobic mesogens that are terminated with different alkyl chains and functional substituents, such as alcohol (for PAH-6), ester (for PAH-2 and PAH-3), carboxylic acid (for PAH-4 and PAH-5), etc. PAH-B, PAH-C, PAH-1, PAH-2 and PAH-6 contain a PAH aromatic core (with a carbon number of 42), whereas PAH-3, PAH-4 and PAH-5 have a semitriangle-shaped aromatic core (with a carbon number of 48) and PAH-A possesses a triangle-shaped core (with a carbon number of 60). These PAH molecules are able to self-assemble into long molecular stacks with a large, electron rich, semiconducting core, which guarantees good charge carrier transport along the molecular stacking direction and a relatively insulated periphery.[21,24−26] Furthermore, the nanometer thick PAH columns can easily form 3D, micrometer sized, spongelike structures with a high surface-to-volume ratio.[20]

Preparation of PAH Films. PAH-A, PAH-C, PAH-1, PAH-2, PAH-3, and PAH-6 solutions were prepared at 1×10^{-3} M concentration in toluene. PAH-4 and PAH-5 solutions were prepared at 1×10^{-3} M concentration in tetrahydrofuran (THF). PAH-B was prepared at 1×10^{-3} M concentration in xylene. For spectroscopic
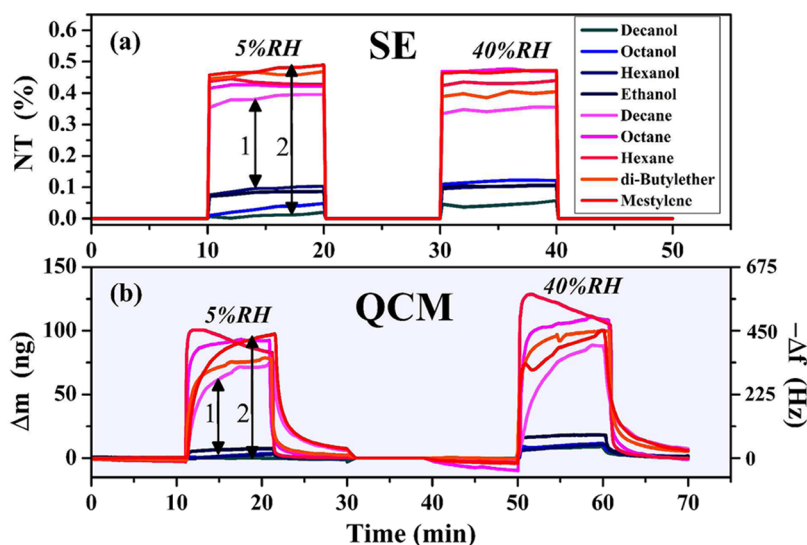
Figure 2. (a) Thickness changes of the **PAH-A** film measured by SE ($NT = \Delta T/T_0$, where ΔT stands for the change in the thickness and T_0 stands for the film's thickness before exposure) upon exposure to various polar and nonpolar analytes in the presence of different humidity contents. (b) Changes in frequency ($-\Delta f$; right y-axis) of a QCM that is disturbed by the addition or removal of a small mass (Δm; left y-axis) at the surface of the acoustic resonator upon exposure to various polar and nonpolar analytes in the presence of different humidity contents.[10] The polar analytes are represented in green and blue, whereas the nonpolar analytes are represented in red, orange, and pink. The gap between the signals acquired in the presence of nonpolar and polar analytes (G_{np-p}) is presented by arrow 1 and the range of responses (RR) is presented by arrow 2. G_{np-p} was calculated as lowest response to any nonpolar analyte minus highest response to any polar analyte, while RR as highest response to any of the analytes minus lowest response to any of the analytes.

ellisopmetry (SE) experiments, 100 μL of PAH solution was drop-casted onto planar p-type Si(100) substrate that was coated with a thermally grown 100 nm SiO$_2$ layer. The samples were then slowly dried under ambient conditions for 30 min and subsequently placed in a desiccator and kept under vacuum overnight. This process led to the formation of nearly continuous films, with thicknesses ranging between 100 $\pm$ 5 nm and 800 $\pm$ 10 nm. For quartz crystal microbalance (QCM) experiments, 2 μL of PAH solution was drop-casted on gold-plated QCM resonators. The samples were then slowly dried under ambient conditions for 30 min and subsequently placed in a desiccator and kept under vacuum overnight. The deposition process was repeated twice to completely cover the gold electrode with nearly continuous PAH layers.

Exposure to Analytes. Oil-free, purified air, obtained from a compressed air source that had a baseline RH of 5.0 $\pm$ 0.2% and an organic contamination of <0.3 ppm (measured by a commercial PID detector − ppbRAE 3000), was used as a carrier gas for the analytes and as reference gas. The vapors of different analytes or water were produced by bubbling air through their liquid states, using glass bubblers. The analyte saturated vapor was carried out the side arm of the bubbler and diluted with a dilution flow of carrier gas at a flow rate of 0.5−5.0 L/min. The RH of the dilution flow was regulated by mixing dry (5.0 $\pm$ 0.2% RH) and wet (100% RH, coming out of the water bubbler) air flows. In this manner, the partial pressure of analyte vapors could be varied between p_a/p_o = 0.01−0.2 (where p_a stands for the partial pressure of the analyte and p_o stands for the saturated vapor pressure at 21 °C) in an environment of 5% RH to 40% RH, where humidity effects become seriously significant on the sensors performance.[27−33] Unless otherwise stated, we focus our presentation on analytes at p_a/p_o = 0.08 in an environment of either 5% RH or 40% RH.

For testing the effect of ambient humidity on the sensors' responses, binary mixtures of volatile analyte and water vapor were used. Sensing experiments with SE and QCM were performed continuously at 20 $\pm$ 2 °C, using three subsequent exposure cycles: (i) exposure to a dry air flow (5.0 $\pm$ 0.2% RH) for 10 min; (ii) exposure to the analyte of interest at p_a/p_o = 0.01−0.2 in 5% or 40% RH background for 10 min; and (iii) purging the chamber with a flow of dry air for 10 min. All measurements were repeated three times in order to check the

congruency of the results. The analytes used in the experiments were: DI-water that is provided by a commercial water purification system (Easypure II), 1-decanol (Sigma-Aldrich Ltd.), dibutylether (Sigma-Aldrich Ltd.), mesitylene (trimethylbenzene; Sigma-Aldrich Ltd.), 1-hexanol (Fluka Analitical Ltd.), 1-octanol (Fluka Analitical Ltd.), ethanol (Frutarom Ltd.), n-hexane (Frutarom Ltd.), n-decane (Arcos Organics), and n-octane (Merck Schuchardt Ltd.). All analytes had a purity of more than 99%. All measurements were repeated three times in order to check the congruency of the results. The responses of the SE and QCM were satisfactorily reproducible from sample-to-sample ($\pm$2% variance) and from batch-to-batch ($\pm$3% variance). The PAH films exhibited negligible changes over time ($\pm$2% experimental error)—for an extended period of 6−8 months—as well as negligible responses toward fluctuations in temperature ($\pm$2 °C) in the measurement apparatus.

Spectroscopic Ellipsometry (SE). SE is an optical technique used for studying dielectric properties and changes in thin film thicknesses. These properties are calculated from the measurement of changes in the polarization of the light that is reflected from the analyzed sample. In the current study, reflected light spectra were recorded over a range between 250−1700 nm using a variable angle rotating compensator spectroscopic ellipsometer (M-2000U Automated Angle, J. A. Woollam Co., Inc., USA), equipped with a specially designed triangular exposure cell that allowed in situ measurements at 70° incidence angle. The thickness of the SiO$_2$ layer was determined prior to the deposition of the PAH films at three incidence angles (65°, 70°, 75°) on an open sample stage, using tabulated values for the refractive indices of Si and SiO$_2$.[34,35] A three-phase cap-layer/SiO$_2$/Si model was employed to extract the optical constants and the thickness (T) of the PAH layers, using the effective media approximation to account for the inclusion of voids into the PAH layer.[36] SE was employed afterward to monitor the thickness changes of the PAH layers during exposures to the (gaseous) analytes, assuming that the changes in the optical constants are much smaller than the thickness changes - NOTE: This assumption is based on the similar dielectric properties of the organic analytes and the organic cap-layers. Our SE probe had an area of about 1 $\times$ 5 mm^2, and the thickness might vary locally. However, the increase of the average thickness upon exposure to the analytes, measured in

Table 2. Gap between the Signals Provided by Nonpolar and Polar Analytes Exposures (G_{np-p}), and Spread of the Signals Acquired upon Exposure to Nonpolar Analytes of Similar Nature (S_{np}) and Polar Analytes of Similar Nature (S_p)

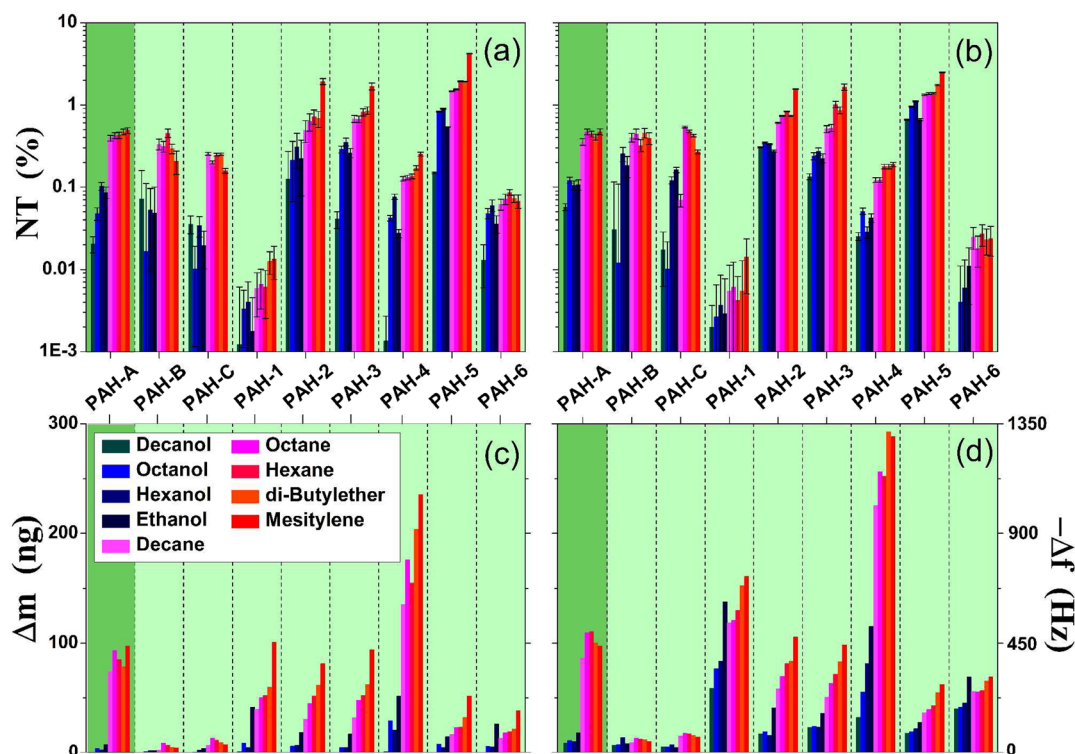|	RH (%)	G_{np-p}	S_{np}	S_p	G_{np-p}/S_{np}	G_{np-p}/S_p
SE (%)	5	0.29 ± 0.05	0.09 ± 0.02	0.08 ± 0.01	3.22 ± 0.48	3.61 ± 0.54
	40	0.23 ± 0.04	0.12 ± 0.02	0.06 ± 0.01	1.89 ± 0.29	3.80 ± 0.57
QCM (ng)	5	65.9 ± 0.4	23.0 ± 0.4	7.8 ± 0.4	2.8 ± 0.1	8.2 ± 0.1
	40	68.1 ± 0.4	24.1 ± 0.4	9.2 ± 0.4	2.8 ± 0.1	7.5 ± 0.1

Figure 3. Thickness changes of the various PAH layers (cf. Figure 1) measured by SE ($NT = \Delta T/T_0$, where ΔT stands for the change in the thickness and T_0 stands for the film's thickness before exposure) upon exposure to various polar and nonpolar analytes (a) 5% RH, and (b) 40% RH; and changes in frequency ($-\Delta f$; right y-axis) of a QCM that is disturbed by the addition or removal of a small mass (Δm; left y-axis) at the surface of the acoustic resonator upon exposure to various polar and nonpolar analytes at (c) 5% RH and (d) 40% RH.[10] The polar analytes are represented in green and blue, whereas the nonpolar analytes are represented in red, orange, and pink. For SE measurements, the error bars for the three repetitions are shown. The error bars in the QCM measurements are not shown because they are negligible (±1 Hz or ±0.2208 ng). Representative reference responses, viz. SE and QCM responses upon exposure to various RH levels without analytes, are presented in the Supporting Information, Figure 1S.

the same place of the sample, can be used as a measure for the amount of analytes adsorbed on the PAH films.

Quartz Crystal Microbalance (QCM). QCM is a piezoelectric mass-sensing device that has the ability to measure very small mass changes, down to a fraction of a monolayer or a single layer of atoms. QCM evaluates a mass per unit area by measuring the change in frequency (δf) of a quartz crystal resonator that is disturbed by the addition or removal of a small mass (Δm) at the surface of the acoustic resonator. The relationship between Δm and δf is described by the Sauerbrey's equation

$$\Delta m = -C_f A \delta f \tag{1}$$

where C_f is the mass sensitivity (= 1.104 ng cm^{-2} Hz^{-1}) and A is the active area of the QCM resonator (= 0.2 cm^2).[11] In the current study, gold-plated QCM resonators (5 mm in diameter; 20 MHz resonant frequency) were used to explore changes in the mass of the PAH sensing films caused by exposures to the (gaseous) analytes. Frequency shifts (δf), before and after exposure to analytes, were recorded by LibraNose 2.1 (Technobiochip, Elba Island, Italy), which is a system composed of a measurement chamber with eight QCM sensors, an internal micropump, and a microelectric valve that conveys the gas samples to the measuring chamber.

3. RESULTS AND DISCUSSION

Figure 2 presents changes in the SE and QCM signals of the PAH-A thin film upon exposure to various polar and nonpolar analytes at p_a/p_o= 0.08, in the presence of different RH conditions in the background. As seen in the figure, exposure of the PAH-A films to various analytes leads to abrupt changes in the SE signals (changes in the thickness of the film; see the Experimental Section). The SE signals stabilize quickly (within 1−2 s) and maintain almost a constant value during the whole exposure period. This behavior is observed regardless the type of the analyte. As for the QCM responses (changes in the adsorbed mass of analytes in/on the film; see the Experimental Section), all nonpolar analytes (excluding hexane) lead to slow changes in the sensing signal, indicating an increase in the mass of adsorbed analyte in/on the PAH-A film. In the case of hexane, a very rapid change in film's mass is produced immediately after the exposure. However, following the rapid/ initial response, a continuous (slight) decrease in the response is obtained. Further securitization of the results presented in Figure 2 shows that the nonpolar analytes exhibit significantly

Table 3. Ratio between *DA* for PAH-A and All Other PAH Films, Based on the Results Obtained in Both SE and QCM Studies

	RH (%)	$DA_{(PAH-A)}/DA_{(PAH-B)}$	$DA_{(PAH-A)}/DA_{(PAH-C)}$	$DA_{(PAH-A)}/DA_{(PAH-1)}$	$DA_{(PAH-A)}/DA_{(PAH-2)}$	$DA_{(PAH-A)}/DA_{(PAH-3)}$	$DA_{(PAH-A)}/DA_{(PAH-4)}$	$DA_{(PAH-A)}/DA_{(PAH-5)}$	$DA_{(PAH-A)}/DA_{(PAH-6)}$
SE	5	1.1 ± 0.2	0.9 ± 0.1	4.0 ± 0.6	6.1 ± 0.9	3.3 ± 0.5	3.1 ± 0.5	4.5 ± 0.7	23.3 ± 3.5
	40	3.7 ± 0.6	−3.2 ± 0.5	12.5 ± 1.9	2.8 ± 0.4	3.5 ± 0.5	1.3 ± 0.2	4.6 ± 0.7	2.2 ± 0.3
QCM	5	26.6 ± 3.5	3.0 ± 0.6	−40.8 ± 5.9	4.8 ± 0.3	4.3 ± 0.2	1.9 ± 0.1	17.1 ± 5.3	−2.0 ± 0.1
	40	−0.9 ± 0.1	1.2 ± 0.1	−3.5 ± 0.1	3.5 ± 0.1	3.4 ± 0.2	1.6 ± 0.1	3.2 ± 0.2	−1.4 ± 0.1

higher signals than the polar analytes for both SE and QCM platforms.

From Figure 2, we could calculate important parameters associated with the detection ability of nonpolar analytes, such as the gap between the signals acquired in the presence of nonpolar and polar analytes (G_{np-p}) and the spread of the signals acquired in the presence of analytes of similar nature (S_{np} and S_p for nonpolar and polar analytes, respectively). The extracted values (Table 2) show that G_{np-p} is much higher (1.9 to 8.2 times higher) than either S_{np} or S_p. The values from Table 2 obtained by QCM are similar at both 5 and 40% RH, demonstrating the suitability of the PAH-A for the detection of nonpolar analytes in the presence of counteracting background of 5−40% RH.

Intuitively, the excellent sensitivity of PAH-A toward nonpolar analytes under high counteracting humidity levels (40% RH) could be ascribed to the hydrophobic nature of the film. To examine this hypothesis, the sensing properties of PAH-A were compared with other hydrophobic PAH derivatives (PAH-B and PAH-C) as well as with a series of hydrophilic PAH derivatives (PAH-1−PAH-6). PAH-B and PAH-C contain hydrophobic mesogens terminated with hydrophobic alkyl chains similar in their chemical nature/ structure to those of PAH-A, whereas PAH-1−PAH-6 contain mesogans terminated with hydrophilic functional groups such as hydroxyl and carboxyl; see Figure 1 and Table 1. As seen in Figure 3, the signals acquired by PAH-B, PAH-C, and PAH-1−PAH-6 in the presence of nonpolar analytes are in general slightly higher than the signals acquired in the presence of polar analytes. However, in most cases, the G_{np-p} values are insignificant or even overlap each other. As a matter of fact, only QCM that is coated with PAH-4 could lead to an obvious distinction between the nonpolar and polar analytes. However, increasing the background humidity from 5 to 40% RH increases the G_{np-p} by 133% and the S_p by 151% (see Figure 3c, d). This observation indicates that the PAH-A/QCM is highly affected by the actual humidity background. Furthermore, the nonadditive nature of this humidity effect is difficult to compensate by post-treatment processes.[17]

The ability of the PAH films to discriminate between nonpolar and polar analytes was examined further by dividing the G_{np-p} by the range of responses (RR = highest response to any of the analytes minus lowest response to any of the analytes, i.e., the total spread of the responses to all analytes analyzed), viz.:

$$DA = \frac{G_{np-p}}{RR} \qquad (2)$$

Table 3 shows the ratio between *DA* calculated for PAH-A and all other PAH films considered in this study (i.e., PAH-B, PAH-C, and PAH-1−PAH-6). The fact that almost all values from Table 3 are > |1|, independent of the measurement method and/or background humidity, unequivocally demonstrates that PAH-A is the most suitable material for clear differentiation

between the nonpolar and polar analytes - NOTE: the negative values in Table 3 indicate overlapping between the responses to nonpolar and polar analytes in these cases. The excellent sensitivity of the PAH-A might be ascribed to the preferred dissolution of the nonpolar analytes into the PAH-A film, in comparison to polar analytes.[37,38] The preferred analyte dissolution leads to higher swelling effect (i.e., an increase in the PAH-A film thickness) upon exposure to nonpolar analytes, compared to polar analytes.[19] The low dissolution of the water molecules in the PAH-A's hydrophobic side-terminations prevent the water penetration into the PAH-A film. However, the QCM results demonstrate that the water molecules exist on the PAH-A surface, most probably as a condensed layer. For each analyte, the mass adsorbed on the PAH-A/QCM (proportional to the measured Δm or $-\Delta f$; see the Experimental Section) at 40% RH was higher than that adsorbed at 5% RH (Figure 2). Additionally, the difference between the QCM response at 40% RH and 5% RH was almost constant (within ±8% experimental error) and equivalent to the mass of water layer condensed at the PAH-A/QCM surface. With this in mind, it is reasonable to argue that water molecules are adsorbed on the PAH-A surface, but do not affect the SE signals, due to negligible changes in the PAH-A film thickness and/or refractive index.

Measuring the SE and QCM responses of the PAH-A films upon exposure to different analyte concentrations (see the Experimental Section) revealed a detection limit of 1−10 ppm. This range of detection limits is equivalent to the majority of sensing technologies, but, on the other hand, is lower than other state-of-the-art ones. For example, state-of-the-art nanomechanical oscillators have high detection limits (down to sub-ppb levels),[39,40] but the high costs of fabrication and high-vacuum and low-temperatures required for operation make them currently impracticable to some extent. Additionally, there is a substantial possibility that the high levels of RH neutralize the frequency (changes) produced by the nanomechanical oscillators. Chemiresistors of conducting polymers are simple to implement but the high response to humidity (also, when the humidity coexist in mixtures containing 1−10s ppm of nonpolar VOCs) can be a disadvantage.[41,42] Chemicapacitors are more stable than chemiresistors, but the response to humidity as well as the long times of response and recovery might be a disadvantage.[43] Polymer-coated surface acoustic wave (SAW)[44] or QCM[45] sensors are mostly responsive to humidity and limited to a detection level of few ppm.

4. SUMMARY AND CONCLUSIONS

The results presented in this study evidence excellent detection of nonpolar analytes achieved with a gas-sensitive film made of PAH-A. Even though the results presented here were obtained through empirical observations, we believe that they are extremely useful for important practical applications under counteracting humidity conditions in the range between 5 and

40% RH. As yet, the origin of the sensing mechanism of the studied PAH-A derivative is still puzzling. Studies investigating the sensing properties of PAH molecules whose mesogen's shape and size as well as functional groups are, synthetically, changed systematically, would provide an insight on the sensing mechanism of the PAH-A. Since the hydrophobicity per se cannot explain the obtained results (mainly PAH-A versus PAH-B and PAH-C), studying the self-assembly and morphological properties of the PAH-A is of critical importance. Elucidating the PAH-A discriminative power toward nonpolar analytes under higher humidity (40−100% RH) conditions, where the interference of water molecules is likely higher than in the 5−40% RH region,[27−33] would widen the spectrum of applications of this material under counteracting humidity conditions in the future. The method is simple to apply and interpret, and does not require the use of sophisticated pattern recognition algorithms.

ASSOCIATED CONTENT

Ⓢ Supporting Information

Exposure of PAH-A, PAH-C, and PAH-4 to variable humidity levels, without analytes. This material is available free of charge via the Internet at http://pubs.acs.org.

AUTHOR INFORMATION

Corresponding Author

* hhossam@technion.ac.il.

Author Contributions

‡These authors contributed equally to the paper.

Notes

The authors declare no competing financial interest.

ACKNOWLEDGMENTS

REFERENCES

(1) Tisch, U.; Haick, H. *MRS Bull.* **2010**, *35*, 797−803.

(2) Tisch, U.; Billan, S.; Ilouze, M.; Phillips, M.; Peled, N.; Haick, H. *CML−Lung Cancer* **2012**, *5*, 107−117.

(3) Tisch, U.; Haick, H. *Rev. Chem. Eng.* **2010**, *26*, 171−179.

(4) Peng, G.; Tisch, U.; Adams, O.; Hakim, M.; Shehada, N.; Broza, Y. Y.; Billan, S.; Abdah-Bortnyak, R.; Kuten, A.; Haick, H. *Nat. Nanotechnol.* **2009**, *4*, 669−673.

(5) Peng, G.; Tisch, U.; Haick, H. *Nano Lett.* **2009**, *9*, 1362−1368.

(6) Ionescu, R.; Broza, Y.; Shaltieli, H.; Sadeh, D.; Zilberman, Y.; Feng, X.; Glass-Marmor, L.; Lejbkowicz, I.; Müllen, K.; Miller, A.; Haick, H. *ACS Chem. Neurosci.* **2011**, *2*, 687−693.

(7) Barash, O.; Peled, N.; Tisch, U.; Bunn, P. A.; Hirsch, F. R.; Haick, H. *Nanomedicine* **2012**, *8*, 580−589.

(8) Barash, O.; Peled, N.; Hirsch, F. R.; Haick, H. *Small* **2009**, *5*, 2618−24.

(9) Rock, F.; Barsan, N.; Weimar, U. *Chem. Rev.* **2008**, *108*, 705−725.

(10) Dickert, F. L.; Geiger, U.; Lieberzeit, P.; Reutner, U. *Sens. Actuat. B* **2000**, *70*, 263−269.

(11) Paska, Y.; Stelzner, T.; Assad, O.; Tisch, U.; Christiansen, S.; Haick, H. *ACS Nano* **2012**, *6*, 335−345.

(12) Paska, Y.; Haick, H. *ACS Appl. Mater. Interface* **2012**, *4*, 2604−2617.

(13) Paska, Y.; Stelzner, T.; Christiansen, S.; Haick, H. *ACS Nano* **2011**, *5*, 5620−5626.

(14) Haick, H. *J. Phys. D* **2007**, *40*, 7173−7186.

(15) Angione, M. D.; Pilolli, R.; Cotrone, S.; Magliulo, M.; Mallardi, A.; Palazzo, G.; Sabbatini, L.; Fine, D.; Dodabalapur, A.; Cioffi, N.; Torsi, L. *Mater. Today* **2011**, *14*, 424−433.

(16) Crowe, L. L.; Solntsev, K. M.; Tolbert, L. M. *Langmuir* **2007**, *23*, 6227−6232.

(17) Konvalina, G.; Haick, H. *ACS Appl. Mater. Interface* **2012**, *4*, 317−325.

(18) Zilberman, Y.; Ionescu, R.; Feng, X.; Mullen, K.; Haick, H. *ACS Nano* **2011**, *5*, 6743−6753.

(19) Zilberman, Y.; Tisch, U.; Shuster, G.; Pisula, W.; Feng, X.; Mullen, K.; Haick, H. *Adv. Mater.* **2010**, *22*, 4317−4320.

(20) Zilberman, Y.; Tisch, U.; Pisula, W.; Feng, X.; Mullen, K.; Haick, H. *Langmuir* **2009**, *25*, 5411−5416.

(21) Feng, X. L.; Liu, M. Y.; Pisula, W.; Takase, M.; Li, J. L.; Müllen, K. *Adv. Mater.* **2008**, *14*, 2684−2689.

(22) Kastler, M.; Pisula, W.; Wasserfallen, D.; Pakula, T.; Müllen, K. *J. Am. Chem. Soc.* **2005**, *127*, 4286−4296.

(23) Stabel, A.; Herwig, P.; Müllen, K.; Rabe, J. P. *Angew. Chem., Int. Ed.* **1995**, *34*, 1609−1611.

(24) Feng, X. L.; Pisula, W.; Zhi, L. J.; Takase, M.; Müllen, K. *Angew. Chem., Int. Ed.* **2008**, *47*, 1703−1706.

(25) Feng, X. L.; Pisula, W.; Kudernac, T.; Wu, D. Q.; Zhi, L. J.; De Feyter, S.; Müllen, K. *J. Am. Chem. Soc.* **2009**, *131*, 4439−4448.

(26) Feng, X. L.; Marcon, V.; Pisula, W.; Hansen, M. R.; Kirkpatrick, J.; Andrienko, D.; Kremer, K.; Müllen, K. *Nat. Mater.* **2009**, *8*, 421−426.

(27) Yan, H.-Q.; Liu, C.-C. *Sens. Actuators, B* **1993**, *10*, 133−136.

(28) Zarnik, M. S.; Belavic, D. *Metrol. Meas. Syst.* **2012**, *XIX*, 133−140.

(29) Bouhadid, M.; Redon, N.; Plaisance, H.; Desbrieres, J.; Reynaud, S. *Macromol. Symp.* **2008**, *268*, 9−13.

(30) Bai, Z.; Xiea, C.; Hu, M.; Zhang, S.; Zeng, D. *Mater. Sci. Eng.* **2008**, *149*, 12−17.

(31) Belghachi, A.; Collins, R. A. *J. Phys. D* **1990**, *23*, 223−227.

(32) Eaton, K.; Douglas, P. *Sens. Actuators, B* **2002**, *82*, 94−104.

(33) Vlachos, D. S.; Skafidas, P. D.; Avaritsiotis. *Sens. Actuators, B* **1995**, *24−25*, 491−494.

(34) Aspnes, D. E.; Theeten, J. B. *J. Electrochem. Soc.* **1980**, *127*, 1359−1365.

(35) Philipp, H. R., *Handbook of Optical Constants of Solids*; Academic Press: Orlando, FL, 1985.

(36) Leinfellner, N.; Ferré-Borrull, J.; Bosch, S. *Microelectron. Rel.* **2000**, *40*, 873−875.

(37) Bennett, M. E.; Alexander, W. A.; Lu, J. W.; Troya, D.; Morris, J. R. *J. Phys. Chem. C* **2008**, *112*, 17272−17280.

(38) Li, B.; Lambeth, D. N. *Nano Lett.* **2008**, *8*, 3563−3567.

(39) Ekinci, K. L.; Huang, X. M. H.; Roukes, M. L. *Appl. Phys. Lett.* **2004**, *84*, 4469−4471.

(40) Ekinci, K. L.; Yang, Y. T.; Roukes, M. L. *J. Appl. Phys.* **2004**, *95*, 2682−2689.

(41) Gardner, J. W.; Bartlett, P. N. *Electronic Noses: Principles and Applications*; Oxford University Press: Oxford, U.K., 1999.

(42) Faglia, G.; Bicelli, F.; Sberveglieri, G.; Maffezzoni, P.; Gubian, P. *Sens. Actuat. B* **1997**, *B44*, 517−520.

(43) Patel, S. V.; Mlsna, T. E.; Fruhberger, B.; Klaassen, E.; Cemalovic, S.; Baselt, D. R. *Sens. Actuators, B* **2003**, *B96*, 541−553.

(44) Yu, H.; Xu, L.; Cao, M.; Chen, X.; Wang, P.; Jiao, J.; Wang, Y. *Proc. IEEE Sens.* **2003**, *2*, 1333−1337.

(45) Di Natale, C.; Macagnano, A.; Martinelli, E.; Paolesse, R.; D'Arcangelo, G.; Roscioni, C.; Finazzi-Agro, A.; D'Amico, A. *Biosens. Bioelectron.* **2003**, *18*, 1209−1218.